Hindawi
Advances in Civil Engineering
Volume 2018, Article ID 8462746, 12 pages
https://doi.org/10.1155/2018/8462746

Research Article

Deformation Monitoring and Stability Analysis of Shaft Lining in Weakly Cemented Stratum

Xianzhou Lyu and Weiming Wang

[1]*College of Architecture and Civil Engineering, Shandong University of Science and Technology, Qingdao 266590, China*

Correspondence should be addressed to Weiming Wang; wang@sdust.edu.cn

Received 8 February 2018; Accepted 9 September 2018; Published 26 December 2018

Academic Editor: Damien Rangeard

Shaft linings in thick weakly cemented stratum have the disadvantages of large deformation and repeated damage after repair. Considering the typical geologic characteristics and the failure characteristics of shaft linings, we establish a multilayer automatic deformation monitoring system in this paper, and the monitoring system can realize the real-time, continuous, and long-term dynamic monitoring on shaft linings. Based on the concrete strength failure criterion under biaxial compression and the analytical solution for spatially axisymmetric problem of thick-wall cylinders, the damage limit of the shaft lining in Xieqiao coal mine is obtained. Then, we choose three sections as the test area according to the typical damage forms of shaft linings to carry out the monitoring scheme on the auxiliary shaft in Xieqiao coal mine. The monitoring results show that the extreme value of the shaft lining deformation is 2.369 mm. And the shaft lining located in the border between the floor aquifer and the bedrock generates the most severe deformation, which is about 89.4% of the deformation limit. The shaft lining deformation increment fluctuates in certain range, which belongs to elastic deformation. Finally, we inverse the stress state according to the deformation value of the shaft lining, and the obtained additional stress is found to be lower than the ultimate compressive strength. Long-term project practice confirms that the deformation monitoring results can reflect the real stress condition of the shaft lining and that the monitoring system can realize the real-time dynamic evaluation for the status of the shaft lining.

1. Introduction

The surface soil of weakly cemented stratum is usually a deep, loose sedimentary layer that is mostly composed of the Tertiary and Quaternary unconsolidated sediment, while the bedrock section is mainly sand layer that is rich in water and low in rock strength [1–3]. Under the action of the aquifer seepage compressive deformation, the covering soil is more prone to water-losing compression deformation [4, 5]. Therefore, the coupling effects of creep and damage of concrete and rock mass, formation seepage and freeze-thaw effect can lead to fatigue accumulation of shaft linings, and cause their overlarge local deformation. Then, the annular fracture zone is formed due to the damage accumulation of the concrete lining. As time goes by, the accumulation of disaster conditions will finally induce the occurrence of geological disasters. For example, in 1995, an accident happened at the twenty-year-old west airshaft in Xinglongzhuang coal mine. The stone of the lining was sheared along the stripping surface, and the peeling heights reached 100~200 mm. What was worse, the transverse reinforcement was exposed, and the cracks water inflow reached 20 m^3/h, which caused an economic loss of millions of RMB [6]. According to incomplete statistics [7, 8], over one hundred shaft linings have ruptured (damaged) in China since 1980s. However, shaft linings are usually in service for a long time before routine maintenance, so that their deformation and destruction are always concealed and abrupt. Once they are damaged, the failure may evolve into a collapsed disaster, bringing huge losses of lives and property.

The prediction and evaluation of the deformation and failure of shaft linings have an important significance for

effectively avoiding special engineering geological disasters in mines. One effective way is to establish mathematical models and numerical simulation models to predict the fracture limit of shaft linings. For example, Liu et al. proposed a nonlinear prediction and discrimination method for the nonmining fracture of shaft linings [9, 10]. Based on combination technology, Shao and Zhang established a KNN prediction model for the deformation and failure of shaft linings, and the model was verified with testing data [11]. Considering the multiple factors of shaft deformation damage, Yuan et al. established a genetic algorithm-support vector machine model for the nonmining fracture prediction of shaft linings and provided a new way for the quick and accurate prediction [12]. Taking the elasticity theory as a foundation, Zhang et al. established a mathematical model for the destruction prediction of shaft linings by MATLAB and then carried out forecast analysis on the force distortion of shaft linings [13]. Their results demonstrated that the stress and deformation of shaft linings could be predicted and analyzed by the model. By virtue of the application examples of main shaft, auxiliary shaft, east airshaft, and west airshaft in Xinglongzhuang coal mine, Xu et al. evaluated the shaft safety by the method of the improved experience fitting and the multivariate statistical distance discriminant [14]. In addition, Chen et al. analyzed the stress and strain relationship, the range of plastic zone, the shaft shape, and the time of shaft lining destruction by numerical simulation [15–17]. It is noticed that the deformation and failure of shaft linings in weakly cemented stratum is a gradually varied, dynamic process under comprehensive effects. Hence, both theoretical calculation and numerical simulation methods have some limitations in the prediction of shaft failure. To be specific, in the course of theoretical calculation, a large number of assumptions must be applied to idealize complex problems; while in numerical simulation, some factors such as dynamic disturbance and spatiotemporal effect are usually ignored, which may result in a certain deviation between the calculated results and the actual results.

Microdeformation monitoring, as a dynamic and real-time testing technology, can be an extremely important means for engineering disaster prevention and control [18–22]. Especially, in the field of deformation monitoring, Chai et al. proposed a deformation monitoring method based on the fiber Bragg grating technique and established the strain transfer relationship between fiber Bragg grating and shaft lining [23–26]. Their proposed method can predict the actual stress-deformation and provide a basis for the prediction of shaft failure. Xu et al. set the monitor location through orthogonal tests and achieved the goal of full-depth, multilayer, and intelligent monitoring [27]. However, the information level of shaft lining monitoring in China is still much lower than that of water conservancy, bridge, and other engineering fields. Firstly, the testing environment is complex and harsh, and the requirement for testing accuracy is high for shaft linings. Secondly, there are some uncertainties for the damage location of shaft linings. Thirdly, it is difficult to authentically implement dynamic feedback of the obtained data for the monitoring system due to the lack of intelligence.

Current research shows that there is always a big obvious deformation before the deformation and failure of shaft linings [28, 29]. Hence, based on the comprehensive analysis of formation characteristics and existing engineering practice, in this paper, we establish an intelligent monitoring system for the real-time dynamic monitoring of shaft linings in the weakly cemented stratum. Combined with a theoretical model, we predict the deformation limit value of shaft linings. Furthermore, by virtue of the deformation monitoring system, we grasp the deformation regularity of shaft linings and successfully predict the failure location. It is believed that our work has important significance for shaft lining disaster control in weakly cemented stratum and similar stratum.

2. Characteristics of Weakly Cemented Stratum

Xieqiao Coal Mine is located in Xieqiao Town, Yingshang County, Fuyang City, Anhui Province of China. The thickness of the weakly cemented loose layer (topsoil layer) is 310.5 m, and the bottom aquifer has a thickness of 60 m. The auxiliary shaft was built in 1991, and the design parameters were 772.2 m in depth and 7.6 m in net diameter. The topsoil section of the shaft lining was made of double-layer reinforced concrete sidewall with a thickness of 1.1 to 1.8 m, while the bedrock section was ordinary plain concrete with a thickness of 800 mm.

The bedrock of Xieqiao coal mine is covered by thin Cenozoic loose layer with a thickness of 390.35 to 509.10 m. The main mineral composition of the weakly cemented loose layer is the "secondary mineral" (the products of rock weathering), ranging in the thickness from 50 to 500 m. The loose layer consists of a number of aquifer and aquiclude along the stratum depth, as shown in Table 1.

According to the Mohr–Coulomb criterion [30–32], the main indicators reflecting the strength of rock soil include elastic modulus E, cohesive force c, and internal friction angle φ. As shown in Figure 1, the variation in strength index of saturated clay is not linear with the increase of formation depth in weakly cemented stratum [33]. The strength parameters of the stratum fluctuate up and down with the increase of the depth. That is, the weakly cemented stratum has obvious delamination, and the strengths of different layers are quite different. As a result, there will be a strength difference surface between two layers. Correspondingly, the location with the maximum strength difference along the shaft depth is the most prone to deformation and failure.

3. Deformation Limit of Shaft Linings in Weakly Cemented Stratum

3.1. Ultimate Forced State Response Model for the Deformation Failure of Shaft Linings. According to the characteristics of nonmining deformation failure of shaft linings, it is in the state of three-dimensional stress and its damage is the result of the vertical pressure, radial pressure, and circumferential pressure [34, 35]. The radial pressure of the internal wall is zero, that is, it is in the state of two-dimensional stress. Therefore, the deformation failure of the shaft generally

Table 1: Structural composition of the weakly cemented stratum in Xieqiao mining area.

Stratum	Depth (m)	Stratigraphic distribution	Parameters	Lithology
1st aquifer	26		q = 0.021~0.603 L/s·m	Medium fine powder
1st aquiclude	25		I_P = 17~22	Sandy clay
2nd aquifer	65		q = 0.199~2.73 L/s·m	Medium fine sand
3rd aquifer	175		k = 3.22~12.14 m/d	Medium coarse sand
2nd aquiclude	70		I_P = 18~29	Clay
3rd aquiclude	40		I_P = 20~30	Clay
4th aquifer	50		q = 0.524~1.935 L/s·m	Medium coarse sand
4th aquiclude	20		—	Cemented clay

q is the unit water inflow, K is the permeability coefficient, and I_P is the plasticity index.

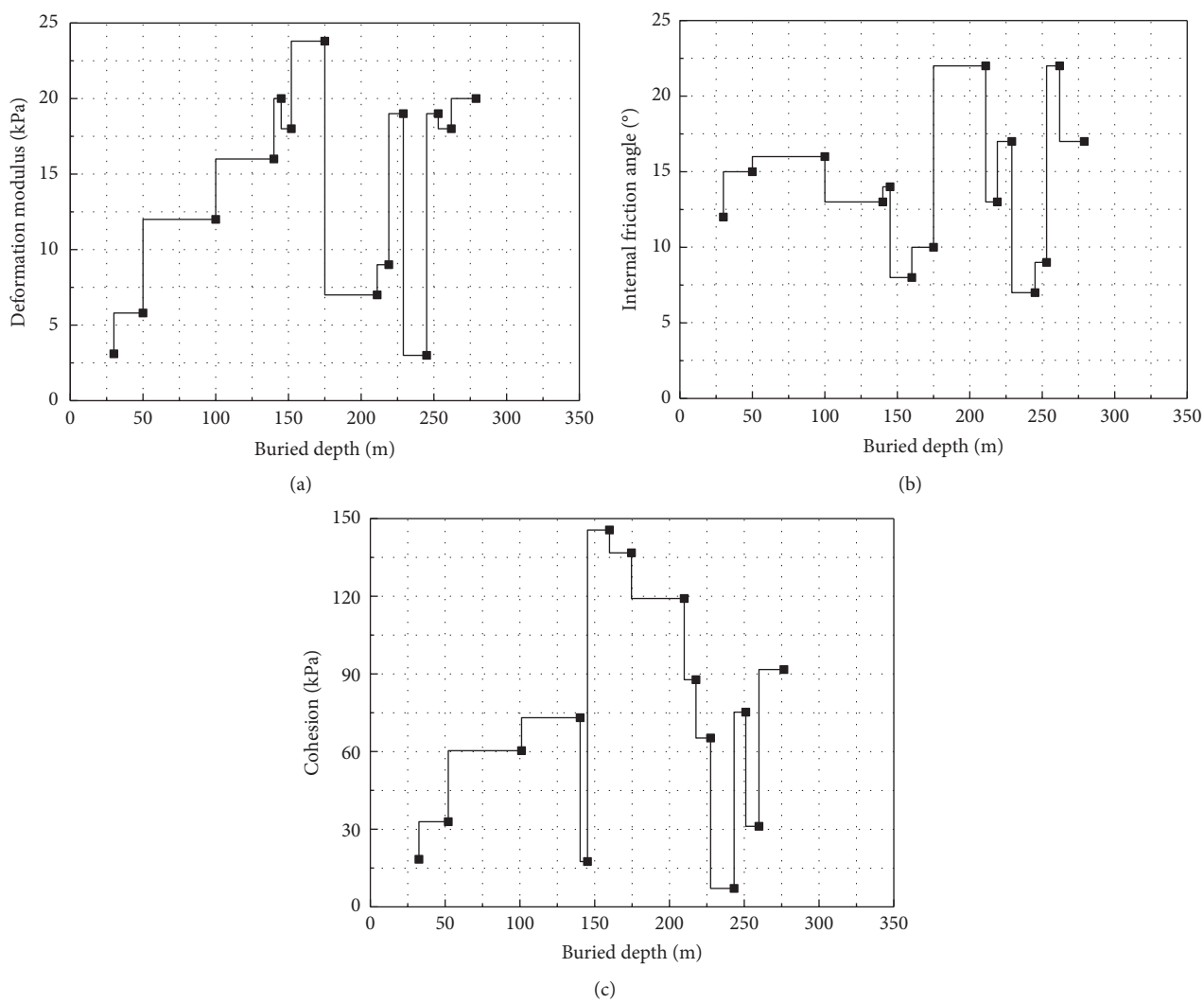

Figure 1: Variation of rock-soil parameters with buried depth. (a) Elastic modulus; (b) friction angle; (c) cohesion.

develops from the internal wall and then gradually extends to the outer wall. When the inner wall ruptures, the exposed shaft lining is still in the state of bidirectional compression. Therefore, the strength failure criterion of concrete under bidirectional load, i.e., the fourth strength theory (energy theory), can be adopted to determine the ultimate state of the shaft lining as shown:

$$\sqrt{\sigma_3^2 + \sigma_2^2 - \sigma_2\sigma_3} \le \sigma_a, \tag{1}$$

where σ_2 is the second principal stress, MPa; σ_3 is the third principal stress, MPa; and σ_a is the design strength of concrete, MPa.

The shaft lining can be assumed to be a spatial axisymmetric thick-wall cylinder with uniformly distributed pressure at both ends and linearly distributed pressure in the longitudinal direction along the depth [36–39], as shown in Figure 2.

For thick-wall cylinders, the uniform load P at the top is

$$P = \frac{u_{r=r_a}E}{\mu r_a} - \frac{2Kr_a r_b^2}{r_b^2 - r_a^2}(H + h), \tag{2}$$

where $u_{r=r_a}$ is the radial displacement; K is the slope of the lateral pressure along the longitudinal distribution, which generally takes 13 kN/m; H is the buried depth of the bottom aquifer; h is the thickness of the bottom aquifer, m; μ is Poisson's ratio of thick-wall cylinders; E is the elastic modulus of thick-wall cylinders; and r_a and r_b are the diameters of inner and external sidewalls, respectively, m. Here, $K = q/H$, where q is the lateral pressure of the lining.

The longitudinal load of the shaft is mainly composed of the deadweight G and the superposition of the additional stress for thick topsoil layer σ_A, namely, $P = \sigma_A + G$. Herein, $G = \gamma_c \cdot H$, where γ_c is the concrete gravity and generally takes 25 kN/m^3. Therefore, the superposition of the additional stress can be obtained as follows:

$$\sigma_A = \frac{u_{r=r_a}E}{\mu r_a} - \frac{2Kr_a r_b^2}{r_b^2 - r_a^2}(H + h) - \gamma_c H. \tag{3}$$

According to existing engineering experience, the border between the floor aquifer and the bedrock segment of the shaft lining in weakly cemented stratum is prone to deformation and failure; that is, the lining located between the topsoil and the bedrock is easiest to be destroyed. The stress state in this region can be expressed as [40]

$$\begin{cases} \sigma_1 = \sigma_{r=r_a} = 0, \\ \sigma_2 = \sigma_\theta \Big| r = r_a = \dfrac{2Kr_b^2}{r_b^2 - r_a^2}h + \dfrac{2qr_b^2}{r_b^2 - r_a^2}, \\ \sigma_3 = \sigma_{z=H+l} = \gamma_c H + \sigma_F, \\ \tau_{r\theta} = 0, \end{cases} \tag{4}$$

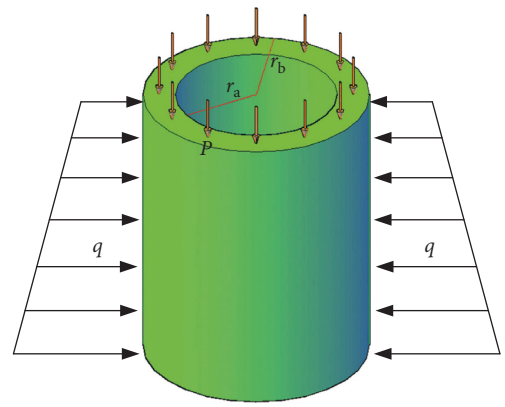

Figure 2: Axisymmetric calculation model of the thick-wall cylinder.

where σ_1, σ_2, and σ_3 are the first, second, and third principal stresses of the shaft lining, respectively, σ_r is the radial stress, σ_θ is the tangential stress, σ_z is the axial stress, and $\tau_{r\theta}$ is the tangential strain.

The limit state means that the internal pressure on the reinforced concrete of internal wall reaches the ultimate compressive strength. Here, the vertical stress σ_z is the vertical ultimate bearing capacity of the internal wall. Thus, it can be seen that

$$\sqrt{\sigma_z^2 + \sigma_\theta^2 - \sigma_z\sigma_\theta} = \sigma_a. \tag{5}$$

When σ_z reaches the largest value,

$$\sigma_z = \frac{\sigma_\theta}{2} \pm \frac{\sqrt{4\sigma_a^2 - 3\sigma_\theta^2}}{2}. \tag{6}$$

Substituting Equation (4) into Equation (6), we can obtain the additional stress of the shaft lining under the limit state, which can be expressed as

$$\overline{\sigma}_A = \frac{Kr_b^2}{r_b^2 - r_a^2}(H + h) + \sqrt{\sigma_a^2 - \frac{3K^2 r_b^4}{\left(r_b^2 - r_a^2\right)^2}(H + h)^2} - \gamma_c H. \tag{7}$$

3.2. Deformation of the Internal Wall of Shaft Linings under the Ultimate Damage. The buried depth of the floor aquifer of the auxiliary shaft in Xieqiao coal mine is 430 m, and the main parameters are shown in Table 2.

Taking the above parameters into Equations (2) and (3), σ_A can be expressed as

$$\sigma_A = 6.003 \times 10^4 u_{r=r_a} - 85.9\,(\text{unit: MPa}). \tag{8}$$

Similarly, according to Equation (7),

$$\overline{\sigma}_A = 56.315\ \text{MPa}. \tag{9}$$

Thus, the deformation value $u_{r=a}$ of the internal wall under the ultimate damage is 2.369 mm.

Table 2: Parameters of the shaft lining in Xieqiao coal mine.

Length (m)	Internal diameter, r_a (m)	Elastic modulus, E (GPa)	Poisson's ratio (μ)	External diameter, r_b (m)	Concrete internal friction angle, φ (°)	Compressive strength, σ_a (MPa)	Concrete density (ρ/kg/m^3)
772.2	3.8	36.5	0.16	5.7	55	60	2500

4. Deformation Monitoring System of Shaft Linings

4.1. Test System. Shaft deformation monitoring system is composed of data acquisition module (multichannel wireless static strain gauge) and sensor system. The data gathered by the data acquisition module are transmitted through wires into static strain gauge. The strain gauge synthesizes and analyzes the data and then transfers them into the computer by wired or wireless modems for further analysis and collection. Based on the real-time monitoring of rock-soil parameters, the system can determine whether the deformation parameters are in the normal working range by analyzing the data variations. The overall arrangement of the test system is shown in Figure 3. The configuration of the test system mainly includes host, JM1900USB bus converter, stabilized voltage supply, displacement sensor, CAT-5E, and system software.

The displacement sensor of the test system adopts the resistive linear displacement sensor. It has the advantages of linearity, high resolution, and little distortion. Its linearity accuracy is 0.3%, and the temperature drift coefficient is 1.5 ppm/°C. Considering the damp and leaking working conditions of the shaft, the displacement sensor uses the waterproof design. The waterproof design mainly includes the air plug type communication cable joint and the silica gel waterproof sleeve, as shown in Figure 4.

4.2. Test System Layout. In recent years, the causes of shaft lining damage have been extensively investigated by many scholars and experts. Through surveying and comparing the damage locations of shaft linings, and considering the typical geological characteristics of the test areas, we set up three monitoring stations (hereinafter referred to as the test areas) at the most dangerous location according to the principles of reducing measurement points, saving costs, focusing on key points, and striving for innovation. The three test areas are the border between the Cenozoic aquifer and the aquiclude (1st test area), the border between the floor aquifer and the bedrock (2nd test area), and the top of the ingate (3rd test area).

Figure 5 shows the inspection station of displacement sensors of the test system and the distribution of substations located in the shaft lining. Considering the hydrological and geological conditions, in order to reduce the testing cost and alleviate the interference on normal working of the shaft lining, we combine the theory research and field test organically so as to reflect the most comprehensive information with the least test parameters. Since the rock stratum inclination is the modest and that the distribution of ground pressure along the shaft lining along the tangential is symmetrical, we adopt the same way for the three test areas. In each test area, four symmetric test points are selected, and the test items include the longitudinal displacement and radial displacement.

Figure 6 shows the layout of the test components. An intelligent control substation detector is set in each test area, which is in charge of the regular testing and timing sampling for the measured point. The measured data will be transmitted to the terminal station on the ground. The terminal station is responsible to send test instructions to each substation, receive the information from the substation, and return the test information to the computer. According to the information feedback analysis, the system can give an alarm in time when a rupture crisis appears.

4.3. Monitoring and Warning Settings. The monitoring system can set the deformation threshold value of the shaft lining according to the deformation limit value obtained by the above theoretical model. After the corresponding sensor exceeds the set alarm threshold value, color or sound alarm will be generated. According to the deformation degree of the shaft lining, two stage warning systems can be set up as shown in Figure 7.

Once the deformation exceeds the upper and lower normal values, the system will blare out a warning; while the deformation exceeds the upper and lower warning values, the system will blare out an alarm.

The monitoring sections of the test system are connected by signal cables along the beam to the ground. The signal transmission of the test system is shown in Figure 8.

5. Deformation Monitoring System Application

Full-depth deformation monitoring of the shaft not only means heavy workload but also needs large economic investment. Therefore, we can select the suitable monitoring sections based on the hydrogeological conditions and the shaft structural characteristics. In this sense, we can achieve the requirement of simple construction economically and reasonably. The Mesozoic stratigraphic break in Xieqiao coal mine and the Cenozoic and Upper Paleozoic is unconformable contact. The total thickness of the upper Paleozoic Permian Shiqianfeng stratum is 127.1 m, in which the weathered fracture zone is 301.5~343.3 m. The below is an intact bedrock segment. The Quaternary loose layer of Cenozoic is a loose sedimentary stratum intersected by the riverbed, floodplain, and shallow lake. Thus, the selected test areas can be depicted as follows (see Figure 9):

(1) The first test area is located in the border between the Cenozoic aquifer and aquiclude, which is 280 m from ground surface in vertical depth. This area is mainly composed of the medium fine sand, coarse

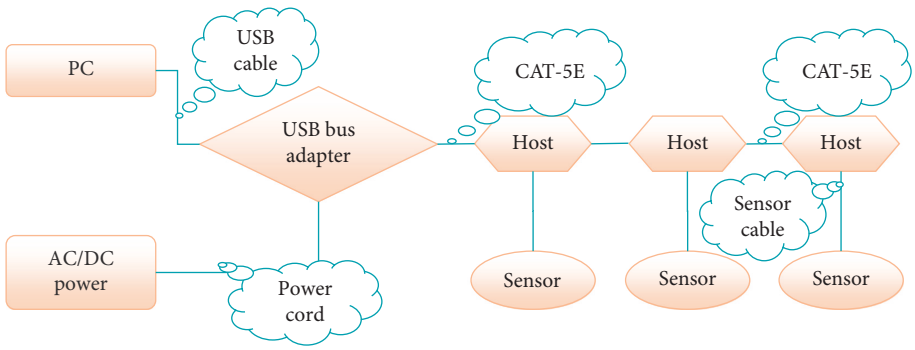

Figure 3: Schematic of the test system.

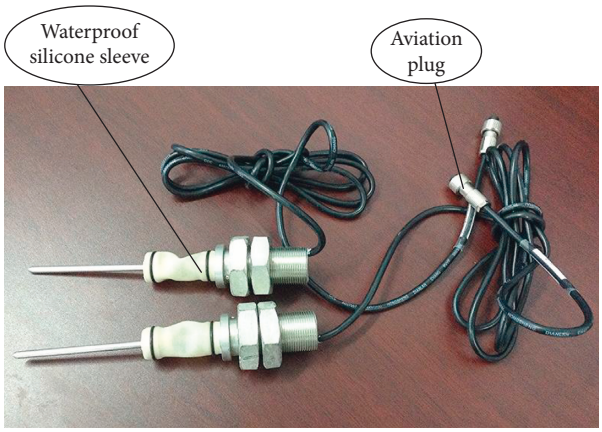

Figure 4: Digital photo of the displacement sensor.

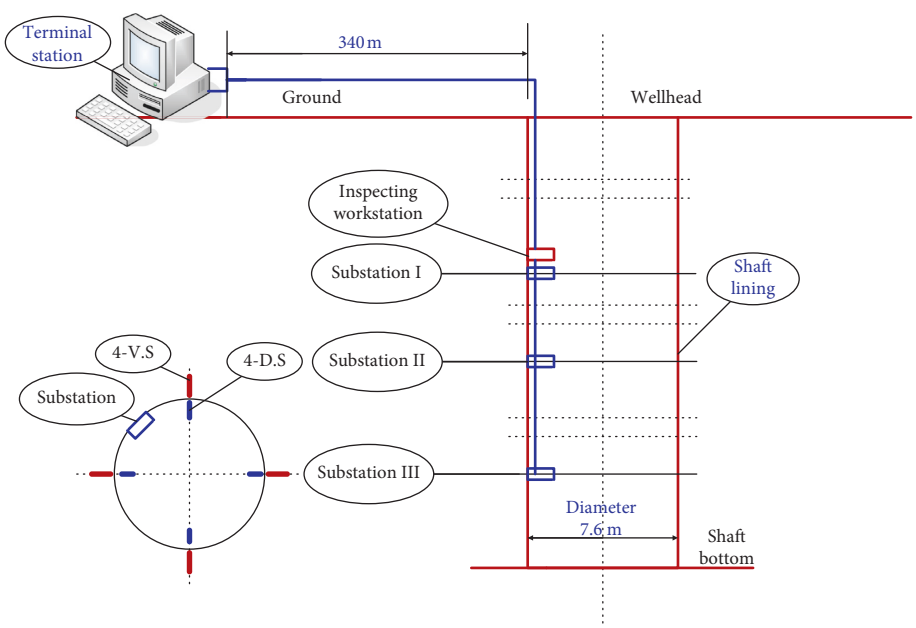

Figure 5: Test system arrangement of the shaft lining.

sand, and multiple layers of gray-green clay and sandy clay.

(2) The second test area is located in the border between the floor aquifer and the bedrock (the location of the large sidewall seat of the shaft lining), which is 430 m from ground surface in vertical depth. The stratum in this area is mainly composed of weathered fine sandstone, clay sand, and weathered mudstone. The

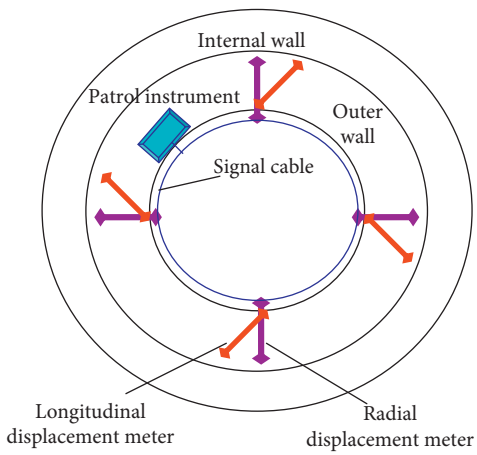

Figure 6: Layout of test components.

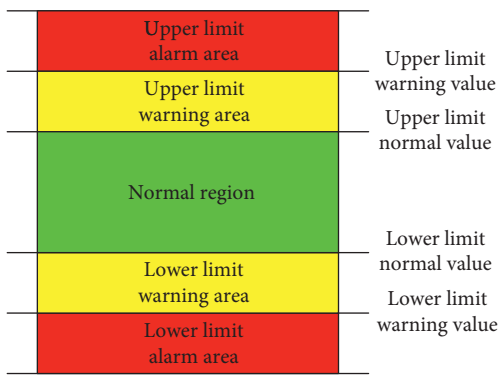

Figure 7: Monitoring warning grading.

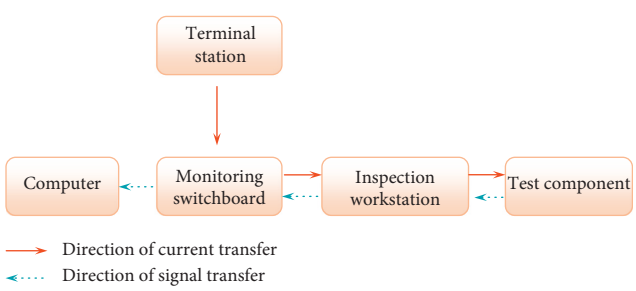

Figure 8: Signal transfer schemes of the test system.

weathered fine sandstone is grayish green clay with thin mudstone. The fracture develops, and the fracture surface is weathered seriously. The weathered mudstone is dark gray, and the cracks are developed.

(3) The third test area is located at the top of the ingate, which is 700 m from ground surface in vertical depth. The stratum in this area is located at the bottom of No. 25 coal seam. It is mainly composed of mudstone, sandstone, as well as locally fine, and medium- and coarse-grained sandstone rock. The rock is compact and moderately stable, and the cracks are undeveloped.

As shown in Figure 9, the test system in Xieqiao coal mine consists of three test areas, and twelve longitudinal and radial displacement sensors. The terminal station is located at the electrical equipment control room, which is about 70 m away from the wellhead. The eight sensors in each section are symmetrically distributed.

The monitoring system can automatically monitor and store the test data for a long time under the control of the computer. The computer in workstation can automatically display (print) the radial and longitudinal displacement reports or the variation curves of the shaft lining through software processing. The ground station staffs can not only analyze and evaluate the condition of the shaft lining in time through the small deformation law given by the computer or report but also share the reports, curves, and analysis results of the shaft lining stability.

6. Deformation Monitoring Results and Shaft Lining Strength Check

6.1. Analysis of Monitoring Results. The deformation monitoring system of the auxiliary shaft in Xieqiao coal mine started running after the installation test in November 2014, and the deformation was monitored in different time periods. In order to analyze the deformation of the shaft lining and evaluate the stability of the monitoring system since the installation of the test system, we process the test data and obtain the longitudinal displacement and radial displacement curves of the shaft lining at different depths.

(i) 1st test area (−280 m)

The test system executes radial and longitudinal displacement monitoring in four directions on the selected three test areas. The sensors numbered 1-1, 1-2, 1-4, and 1-6 are radial displacement sensors, and those numbered 1-3, 1-5, 1-7, and 1-8 are longitudinal displacement sensors, as shown in Figure 9. The deformation of the first test area is shown in Figure 10, where the original point of the number of days in the figure represents 20th November, 2014. As can be seen from the figure, the maximum longitudinal deformation value of the shaft lining is about 1.5 mm and the maximum radial deformation value is about 0.48 mm. The deformation of the shaft lining is within the deformation limit.

(ii) 2nd test area (−430 m)

The test system executes radial and longitudinal displacement monitoring in four directions on the selected three test areas. The sensors numbered 2-2, 2-5, 2-6, and 2-7 are radial displacement sensors, and those numbered 2-1, 2-3, 2-4, and 2-8 are longitudinal displacement sensors, as shown in Figure 9. The deformation of the second test area is shown in Figure 11. As can be seen from the figure, the maximum longitudinal deformation value of the shaft lining is about 1.8 mm and the maximum radial deformation is about 1.95 mm, which are close to the rupture limit. The deformation of shaft lining in this location is the largest, which is about 82.5% of the limit value of shaft lining deformation. Hence, we should pay close attention to strength monitoring of the shaft lining.

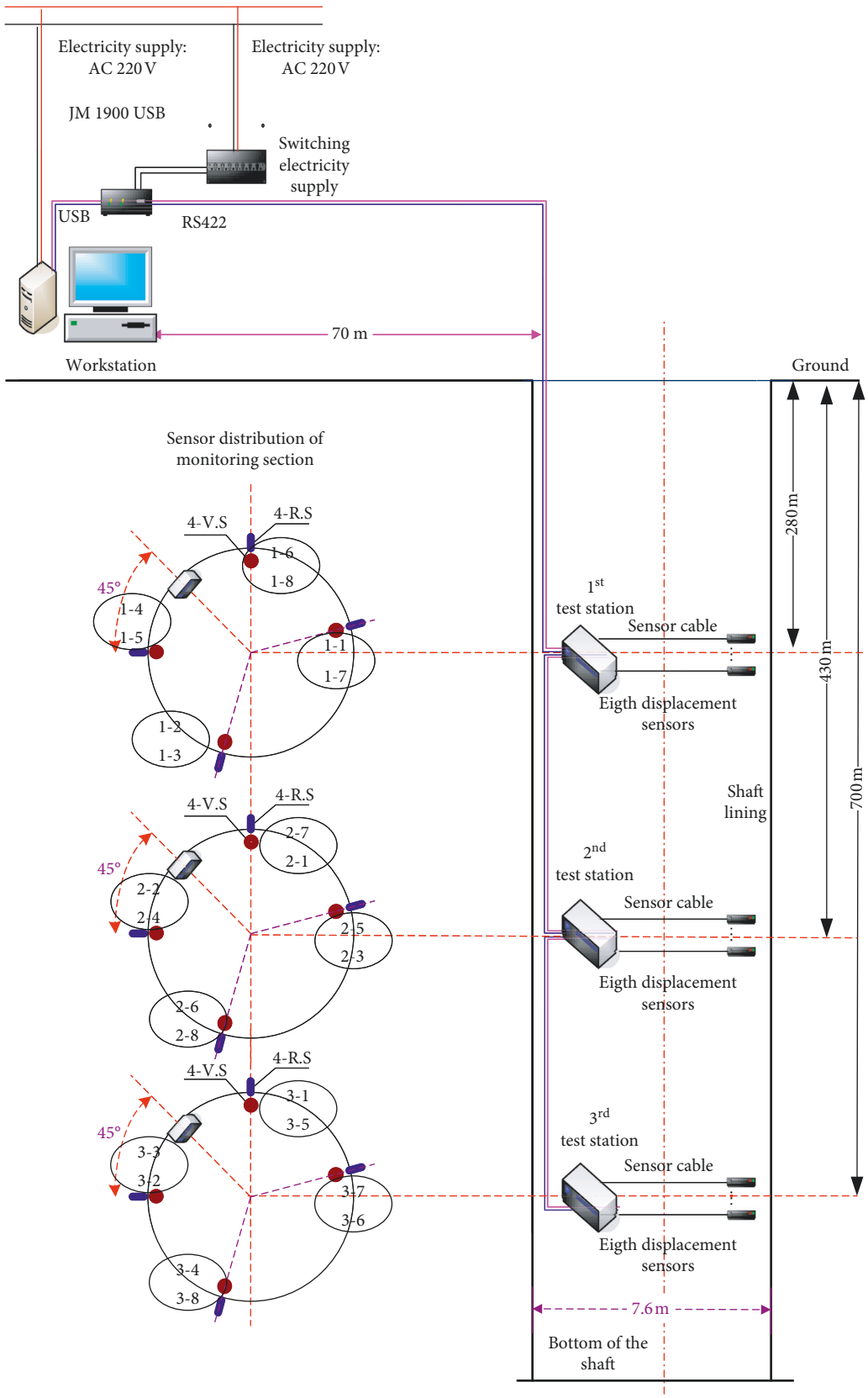

Figure 9: Test system arrangement of the shaft lining in Xieqiao coal mine.

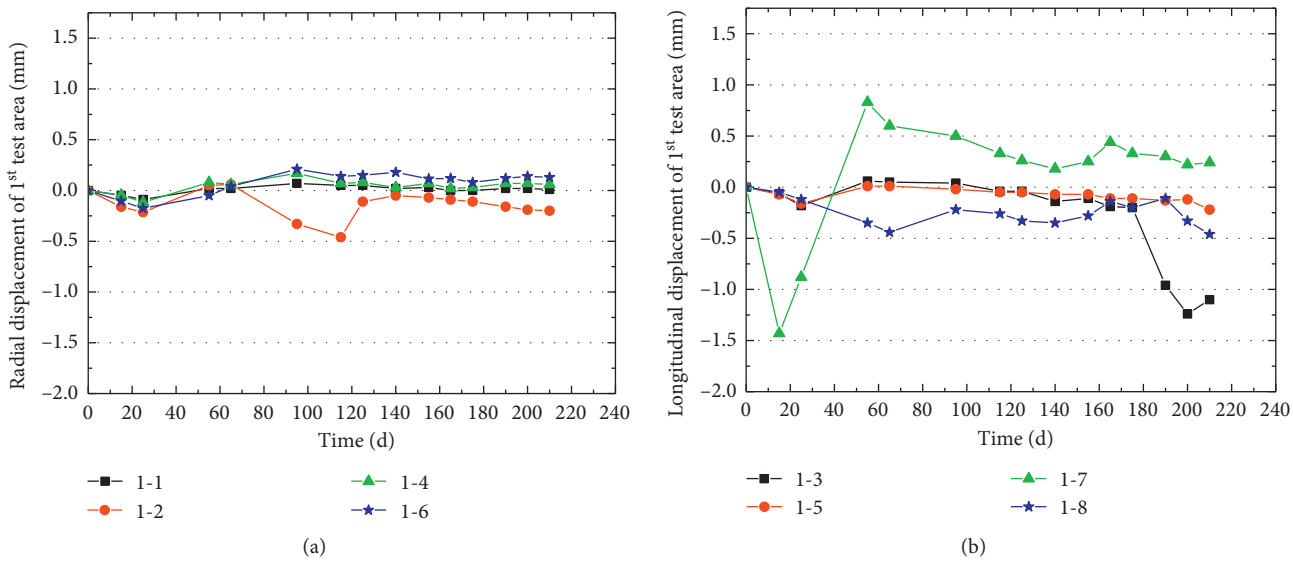

Figure 10: Radial and longitudinal displacement curves at the first test area (−280 m). (a) Radial displacement; (b) longitudinal displacement.

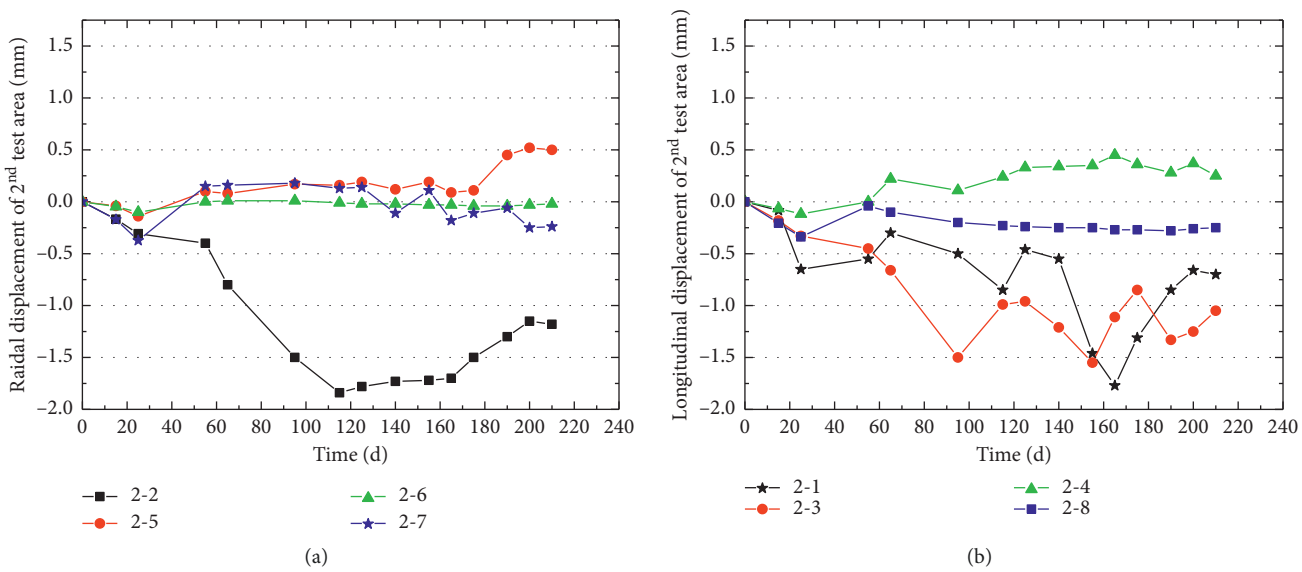

Figure 11: Radial and longitudinal displacement curves at the second test area (−430 m). (a) Radial displacement; (b) longitudinal displacement.

(iii) 3rd test area (−700 m)

The test system executes radial and longitudinal displacement monitoring in four directions on the selected three test areas. The sensors numbered 3-1, 3-3, 3-4, and 3-7 are radial displacement sensors, and those numbered 3-3, 3-5, 3-6, and 3-8 are longitudinal displacement sensors, as shown in Figure 9. The deformation of the third test area is shown in Figure 12. As can be seen from the figure, the maximum longitudinal deformation value of the shaft lining is about 1.12 mm and the maximum radial deformation is about 0.2 mm. The lining deformation is relatively small, and the shaft lining shows good working condition.

In summary, the shaft lining deformation increment fluctuates in certain range, which belongs to elastic deformation. From the deformation curves, we can see that the maximum displacement of the shaft lining appears at the border between the floor aquifer and the bedrock section in weakly cemented stratum. The deformation curves of the shaft lining may reach the peak values within a period of time, so we should pay close attention to the deformation during this period. Therefore, during normal working of the shaft lining, we should strengthen the subtime subregional monitoring and take active control and preventive measures to prevent the occurrence of disasters.

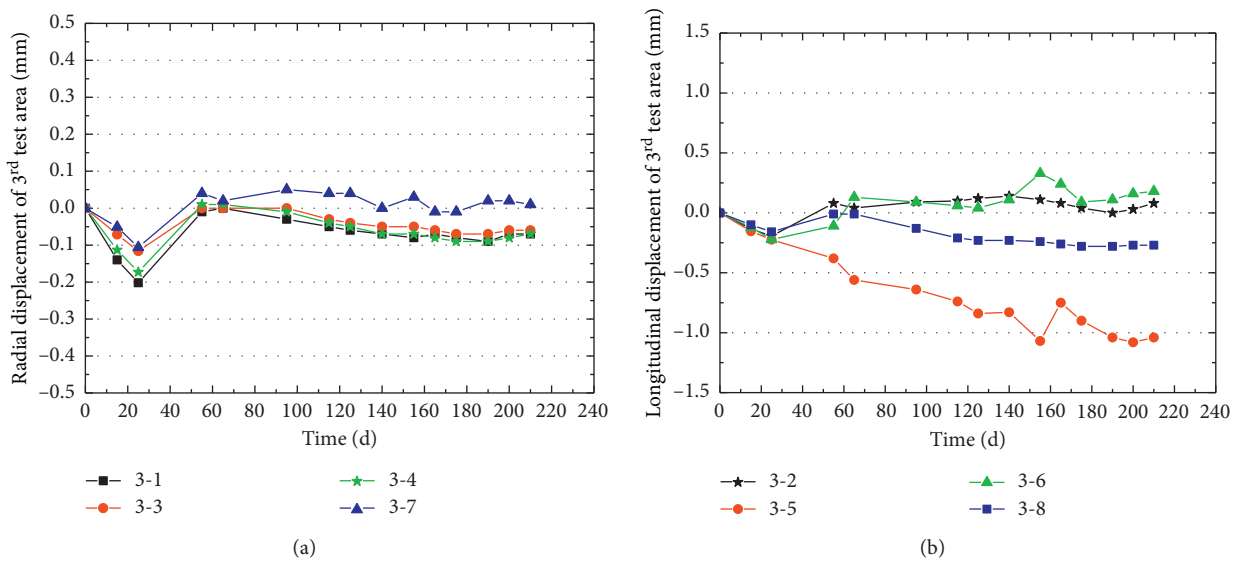

Figure 12: Radial and longitudinal displacement curves at the third test area (−700 m). (a) Radial displacement; (b) longitudinal displacement.

6.2. Shaft Lining Strength Check. The maximum deformation of the shaft lining appears at the border between the floor aquifer and the bedrock, and the radial displacement is 1.95 mm. According to Equation (3), the additional stress at this location is

$$\sigma_A = \frac{u_{r=r_a} E}{\mu r_a} - \frac{2K r_a r_b^2}{r_b^2 - r_a^2}(H + h) - \gamma_c H = 31.15\ \text{MPa} < \sigma_a = 60\ \text{MPa}. \quad (10)$$

Obviously, the shaft lining has not reached the rupture limit. The results show that the deformation and failure of the shaft lining is a step-by-step process. By real-time dynamic monitoring on the deformation of the shaft lining, we can analyze the stress state of the shaft lining by back analysis of the deformation. Thus, the safe state of the shaft lining can be evaluated reasonably.

7. Conclusions

(1) The weakly cemented stratum is obviously stratified, and the strength parameters fluctuate up and down with the depth of the stratum. Therefore, a strength difference surface will be generated between two layers. The sidewall is the most prone to deformation and cause damage at the position where the strength difference in the depth direction is the largest.

(2) According to the strength criterion of two-way compressive concrete and the displacement solution of the axisymmetric problem of thick-wall cylinders, the deformation value of the inner wall of the shaft lining is 2.369 mm.

(3) The intelligent deformation monitoring system of the shaft lining can realize the prediction of multipoint deformation for deep shaft lining. The monitoring results show that the maximum longitudinal and radial deformation values of the shaft lining are about 1.8 mm and 1.95 mm, respectively.

(4) The maximum displacement of the shaft lining appears at the border between the floor aquifer and the bedrock section in weakly cemented stratum. Long-term follow-up monitoring results show that the shaft lining is in good working condition, but the area near the deformation limit should be paid close attention. In addition, it needs to take active control and preventive measures in order to prevent the occurrence of disasters.

(5) The additional stress value at the position of the shaft lining with the maximum deformation is less than the ultimate compressive strength. Therefore, the monitoring results can well reflect the stress state of the shaft lining, and the monitoring system can realize the real-time dynamic intelligent evaluation for the safety state of the shaft lining.

Data Availability

The data used to support the findings of this study are available from the corresponding author upon request.

Conflicts of Interest

The authors declare that they have no conflicts of interest.

Acknowledgments

This paper was supported by the National Natural Science Foundation of China (Nos. 41472280 and 51774196).

References

[1] H. Y. Dai, W. C. Li, Y. X. Liu, and Y.-D. Jiang, "Numerical simulation of surface movement laws under different uncemented layers thickness," *Transactions of Nonferrous Metals Society of China*, vol. 21, pp. s599–s603, 2011.

[2] W. Yang and X. Xia, "Prediction of mining subsidence under thin bedrocks and thick uncemented layers based on field measurement and artificial neural networks," *Computers and Geosciences*, vol. 52, pp. 199–203, 2013.

[3] D. H. Li, G. S. Xu, and H. Z. Yu, "Study on features of surface dynamic movement and deformation caused by coal mining under thick alluvium," *Coal Science and Technology*, vol. 42, no. 7, pp. 103–106, 2014, in Chinese.

[4] H. Y. Liu, W. Z. Chen, and Z. M. Wang, "Theoretical analysis of shaft lining damage mechanism of Yanzhou mine," *Journal of Rock Mechanics Engineering*, vol. 26, no. 1, pp. 2060–2062, 2007, in Chinese.

[5] D. D. Zhang, *Experimental study on seepage and deformation in deep uncemented layer in east China*, Ph.D. thesis, Xi'an University of Science and Technology, Xi'an, China, 2013.

[6] W. Q. Zhang, Y. S. Zhang, J. D. Xi et al., "The mechanism of sidewall cracking in vertical well of coal mine and its prevention countermeasures," *Journal of Geology Hazard Control*, vol. 12, no. 4, pp. 15–19, 2011.

[7] X. H. Ni, W. H. Sui, and Y. Z. Guan, *Summary of Sidewall Cracking in Vertical Well of Coal Mine in China*, China University of Mining and Technology Press, Beijing, China, 2005, in Chinese.

[8] W. H. Yang, "The development and prospect of China's freezing method sinking technology in the pastdecade," in *Proceedings of 50th Anniversary of the China Coal Society*, Beijing, China, November 2012.

[9] H. Y. Liu, X. Li, Q. B. Zeng et al., "The nonlinear methods of forecast and judgment for shaft-lining non-mining fracture of Yanzhou mine," *Journal Engineering Geology*, vol. 13, no. 2, pp. 231–235, 2005, in Chinese.

[10] H. Y. Liu, S. J. Wang, Q. B. Zeng et al., "Judgment for non-mining fracture of shaft-lining in Yanzhou mine based on fuzzy neural network," *Journal of Geotechnical Engineering*, vol. 27, no. 10, pp. 1237–1240, 2005, in Chinese.

[11] L. B. Shao and Y. Zhang, "Forecast for non-mining fracture of shaft-lining of mine," *Journal of China Coal Society*, vol. 34, no. 2, pp. 184–186, 2009, in Chinese.

[12] Z. G. Yuan, H. T. Wang, G. Z. Hu et al., "Forecast model of GA-SVM for shaft-lining non-mining fracture," *Journal of China Coal Society*, vol. 36, no. 3, pp. 393–397, 2011, in Chinese.

[13] X. D. Zhang, Y. D. Han, S. J. Liu et al., "Deformation prediction analysis model for the mine shaft-wall," *Journal of Liaoning Technical University (Natural Science)*, vol. 33, no. 8, pp. 1070–1073, 2014, in Chinese.

[14] Y. C. Xu, Y. B. Gao, J. H. Li et al., "Improvement and application of mine shaft safety evaluation system," *Coal Science and Technology*, vol. 44, no. 10, pp. 95–101, 2016, in Chinese.

[15] X. F. Chen, M. L. Shen, Y. Zhang et al., "Numerical model research of super deep shaft sidewall destruction," *Journal of Underground Space and Engineering*, vol. 5, pp. 926–931, 2010, in Chinese.

[16] C. W. Wang, "The research of auxiliary shaft's failure mechanism and deformation," Master thesis, AnHui University of Science and Technology, Huainan, China, 2015, in Chinese.

[17] H. Zhang, "Study on the deformation mechanism of shaft lining of Qianyingzi coal Mine in Su-Nan mining area," Master thesis, China University of Mining and Technology, Xuzhou, China, 2016, in Chinese.

[18] S. Baselga, P. Garrigues, J. L. Berné, A. B. Anquela, and A. Martín, "Deformation monitoring in historic buildings: a case study," *Survey Review*, vol. 43, no. 323, pp. 484–492, 2011.

[19] J. Chen, T. Wang, Y. Zhou, Y. Zhu, and X. Wang, "Failure modes of the surface venthole casing during longwall coal extraction: a case study," *International Journal of Coal Geology*, vol. 90–91, pp. 135–148, 2012.

[20] Y. Kalkan, "Geodetic deformation monitoring of Ataturk dam in Turkey," *Arabian Journal of Geosciences*, vol. 7, no. 1, pp. 397–405, 2014.

[21] V. D. Baryshnikov, D. V. Baryshnikov, L. N. Gakhov, and V. G. Kachal'sky, "Practical experience of geomechanical monitoring in underground mineral mining," *Journal of Mining Science*, vol. 50, no. 5, pp. 855–864, 2014.

[22] V. N. Oparin, V. F. Yushkin, G. N. Polyankin, A. N. Grishin, A. O. Kuznetsov, and D. E. Rublev, "Geomechanical monitoring of temporal lining in railway tunneling in complex geological conditions," *Journal of Mining Science*, vol. 51, no. 5, pp. 839–859, 2015.

[23] J. Chai, J. X. Liu, B. Qiu et al., "Detecting deformations in uncompacted strata by fiber Bragg grating sensors incorporated into GFRP," *Tunnelling and Underground Space Technology*, vol. 26, no. 1, pp. 92–99, 2011.

[24] B. Qiu, "Study on the prediction of shaft deformation with huge uncemented soil layer based on FBG monitoring," Master thesis, Xi'an University of Science and Technology, Xi'an, China, 2009, in Chinese.

[25] H. K. Liu, "The research of monitoring and early warning method and system for shaft deformation based on the technology of FBG," Doctoral dissertation, Beijing Jiaotong University, Beijing, China, 2014.

[26] M. L. Huang, B. Wu, and H. K. Liu, "The development of shaft monitoring and early warning system based on the technology of FBG," *Civil Engineering Journal*, vol. 48, no. 1, pp. 424–428, 2015, in Chinese.

[27] L. N. Xu, W. M. Wang, and B. S. Wang, "Shaft safety monitoring warning system," *Mine Construction and Technology*, vol. 24, no. 1, pp. 27–29, 2003, in Chinese.

[28] H. C. Liang, G. H. Zhou, G. S. Zhao et al., "Strain characters of shaft lining crack," *Journal Coal Society*, vol. 35, no. 2, pp. 198–202, 2010, in Chinese.

[29] X. X. Chen and W. H. Yang, "Experimental study of horizontal ultimate loading capacity of new type monolayer freezing shaft lining," *Journal of Rock Mechanics and Engineering*, vol. 32, no. 2, pp. 3740–3748, 2013, in Chinese.

[30] M. Singh, A. Raj, and B. Singh, "Modified Mohr–Coulomb criterion for non-linear triaxial and polyaxial strength of intact rocks," *International Journal of Rock Mechanics and Mining Sciences*, vol. 48, no. 4, pp. 546–555, 2011.

[31] H. C. Biscaia, C. Chastre, and M. A. G. Silva, "Modelling gfrp-to-concrete joints with interface finite elements with rupture based on the Mohr-coulomb criterion," *Construction and Building Materials*, vol. 47, pp. 261–273, 2013.

[32] N. Barton, "Shear strength criteria for rock, rock joints, rockfill and rock masses: problems and some solutions," *Journal of Rock Mechanics and Geotechnical Engineering*, vol. 5, no. 4, pp. 249–261, 2013.

[33] Y. C. Xu, "Mechanics characteristics of deep saturated clay," *Journal Coal Society*, vol. 29, no. 1, pp. 26–30, 2004, in Chinese.

[34] G. S. Zhao, G. Q. Zhou, G. R. Zhong, F. P. Zhu, and H. C. Liang, "Analysis of stratum grouting influence on shaft lining stress with the methods of simulation and in site measurements," *Procedia Earth and Planetary Science*, vol. 1, no. 1, pp. 497–502, 2009.

[35] Z. Q. Meng, H. G. Ji, and F. Peng, "Additional stress of shaft linings in thick alluvium constructed by freezing process," *Journal Coal Society*, vol. 38, no. 2, pp. 204–208, 2013, in Chinese.

[36] Y. Zhou and G. Q. Zhou, "Axisymmetric deformation analysis for the double layer shaft with a plastic interlayer," *Journal Coal Society*, vol. 35, no. 9, pp. 1470–1475, 2010, in Chinese.

[37] Y. Zhou, G. Q. Zhou, and H. Q. Liang, "Mechanical analysis of a restricting inside lining used in the shaft-curing method," *Journal of China University of Mining and Technology*, vol. 38, no. 2, pp. 197–2020, 2009, in Chinese.

[38] H. Y. Liu, "The study of development mechanism and harnessing technology for shaft fracturing in thick alluvim," Doctoral dissertation, HoHai University, Nanjing, China, 2005, in Chinese.

[39] Y. P. Liang, H. Z. Wang, and X. M. Ren, "Analytical solution of axisymmetric problem of thick walled cylinder subjected to uniform and axial linear distribution of pressure at both ends," *Science in China (Series G: Physics, Mechanics and Astronomy)*, vol. 37, no. 5, pp. 684–688, 2007, in Chinese.

[40] H. B. Jia, "Analysis forecast on deformation and failure of non-mining in thick alluvium shaft," Master thesis, Shandong University of Science and Technology, Qingdao, China, 2010, in Chinese.